

# Synthesis and Characterization of Mullites From Silicoaluminous Fly Ash Waste


Virendra K. Yadav, Jaipur National University, India

Pallavi Saxena, Mohanlal Sukhadiya University, India

Chagan Lal, Harcourt Butler Technical University, India

Govindhan Gnanamoorthy, University of Madras, India

Nisha Choudhary, Central University of Gujarat, India

 <https://orcid.org/0000-0002-1847-6520>

Bijendra Singh, Central University of Gujarat, India

Neha Tavker, Central University of Gujarat, India

Haresh Kalasariya, Sankalchand Patel University, India

Pankaj Kumar, Central University of Gujarat, India

## ABSTRACT

Fly ash is considered one of the major hazardous pollutants around the globe. Every year a million tonnes of fly ash is disposed of into the fly ash ponds which are major sites of pollution. The major fractions of fly ash are silicates, aluminates, and ferrous substances followed by minor traces element oxides. The aluminates and silicates comprise of 70% of the fly ash. The aluminates and silicates are present in fly ash in the form of crystalline mullites and sillimanites. Mullites being inert and crystalline are retractile to mineral acids. So, here the authors have reported a novel and simple step for the recovery of all the major elements of fly ash along with recovery of mullites by using hydrofluoric acid at room temperature. The method comprises of treatment of fly ash with diluted hydrofluoric acid for 12 hours under agitation. The recovered white color mullite powder, rod shaped of size 90-300 nm, was analyzed by the sophisticated instruments for the confirmation of the mullite particles.

## KEYWORDS

Aluminosilicate, Fly Ash, Mullites, Refractile, Sillimanites

## 1. INTRODUCTION

Mullite is an exceptionally advanced solid solution of aluminum silicate ( $3\text{Al}_2\text{O}_3 \cdot 2\text{SiO}_2$ ), which is developed by the sintering of rare raw minerals that consists of alumino-silicate under extreme temperature and low pressure (Wang & Sacks, 2005). Mullites are crystalline compositions prominently, comprising of elements like Al, Si, and O (H. Schneider, R. Fischer, & J. Schreuer, 2015a). They are non-stoichiometric compounds structurally similar to impure magnetite which belong to the compositional series of orthorhombic alumino-silicates with the general composition  $\text{Al}_2(\text{Al}_{2+2x}\text{Si}_{2-2x})\text{O}_{10-x}$  (Li & Thomson, 1991)(Fischer, Gaede-Köhler, Birkenstock, & Schneider, 2012). They usually

DOI: 10.4018/IJANR.20200101.oa2

This article published as an Open Access article distributed under the terms of the Creative Commons Attribution License (<http://creativecommons.org/licenses/by/4.0/>) which permits unrestricted use, distribution, and production in any medium, provided the author of the original work and original publication source are properly credited.

exhibit two stoichiometric forms, i.e.  $3\text{Al}_2\text{O}_3\cdot 2\text{SiO}_2$  or  $2\text{Al}_2\text{O}_3\cdot \text{SiO}_2$  and can be characterized by using high-end techniques like X-ray diffraction (XRD) and Scanning electron microscope (SEM) in the fly ash (Y. Gong, Sun, Sun, Lu, & Zhang, 2019). Mullites are found in high temperature metamorphosed rocks of the sanidinite and clay (Laita, Bauluz, & Yuste, 2019). They are also known as “porcelainite” as they are moulded under extremely high temperature using clay (Tripathi, Ghosh, Halder, Mukherjee, & Maiti, 2012). Among the minerals, mullites are also found in hornfels rock (porcellanite) (Searle, 1962), e.g., at the point of contact of bauxites with olivine dolerite intrusions. Special and rare occurrences of mullite are in aluminosilicate lechatelierite glasses produced by lightening impact in sandstones (Pasek, Block, & Pasek, 2012). In addition to this, mullites presence can also be found in small druses of volcanic rocks (e.g., in the Eifel mountain, Western Germany), where it probably grew under moderate hydrothermal conditions (H. Schneider, Schreuer, & Hildmann, 2008).

They own magnificent and unique properties in the form of needles in porcelain (Martin-Marquez & Romero, 2010) like low thermal expansion (Oikonomou, Dedeloudis, Stournaras, & Ftikos, 2007), low thermal conductivity (L. Gong, Wang, Cheng, Zhang, & Zhang, 2014), high thermal and corrosion stability (Baspinar & Kara, 2009), high strength (Liu, 2011), high fracture toughness (Santos & Rodrigues, 2003), excellent creep resistance (Torrecillas et al., 1999), good thermal shock and stress resistance (Uribe, Moreno, & Baudín, 2001), good strength, wear-resistant and useable to high temperatures (H. Schneider, Schmüker, & MacKenzie, 2005). In addition to this, mullite is the only stable binary phase existing system of the  $\text{Al}_2\text{O}_3$ - $\text{SiO}_2$  under ambient conditions (Martin-Marquez & Romero, 2010). Its chemical configurations empirically include 71.8 wt.%  $\text{Al}_2\text{O}_3$  and 28.2 wt.%  $\text{SiO}_2$ , which is designated as 3/2- mullite ( $3\text{Al}_2\text{O}_3\cdot 2\text{SiO}_2$ ) (Ohtake et al., 1991). Moreover, mullite has no charge balancing cations present in them (O'Connor, Mackenzie, Smith, & Hanna, 2010). As a result, there are three different aluminium sites: two distorted tetrahedral and one octahedral (H. Schneider, R. X. Fischer, & J. Schreuer, 2015b). They have two common morphologies: platelet shaped and needle shaped. Platelet shape particles have low aspect ratio while needle shape particles has high aspect ratio. If it forms during the process of sintering, then it provides increased mechanical strength and thermal shock resistance (Chen, Lan, & Tuan, 2000).

Mullite is undoubtedly one of the most imperative oxide material for the both, the conventional and the advanced ceramics (Igo, 2019). Mullite is formed in fly ash during various melting and firing processes, and is used as a refractory material due to its high melting point of 1840 °C (Kamara, Wei, & Ai, 2020). Besides this, due to their distinctive properties, it treasures applications in ceramic whiteware (Sadik, Amrani, & Albizane, 2014; Hartmut Schneider et al., 2015b), porcelains (Anggono, 2005), high-temperature insulating refractory materials (Aksel, 2003), furnace liners (Sadik, El Amrani, & Albizane, 2014), electrical insulators, protection tubes, kiln furniture, rollers, heat exchanger components, heat insulation parts, pressed parts (Eom, Kim, & Raju, 2013) and isostatically pressed parts. It also is utilized as a synthetic analog of mullite that can be an effective standby for platinum in diesel engines (Cui, Zhang, Fu, Wang, & Zhang, 2020; Eom et al., 2013).

The composition of mullite is commonly denoted as  $3\text{Al}_2\text{O}_3\cdot 2\text{SiO}_2$  (71.83 wt. %  $\text{Al}_2\text{O}_3$ ) (T. F. Choo, Mohd Salleh, Kok, Matori, & Abdul Rashid, 2020). However, commercially available mullite which is a solid solution generally consists of 71-76 wt.%  $\text{Al}_2\text{O}_3$ , 23-24 wt. %  $\text{SiO}_2$ , and small quantities of  $\text{TiO}_2$ ,  $\text{Fe}_2\text{O}_3$ ,  $\text{CaO}$ , and  $\text{MgO}$  (T. F. Choo et al., 2020). Stoichiometric ( $3\text{Al}_2\text{O}_3\cdot 2\text{SiO}_2$ ) mullite can be produced without a glassy grain boundary phase that results in an extraordinary strength being maintained at high temperatures (Treadwell, Dabbs, & Aksay, 1996).

The importance and the demand for mullites are progressively increasing day by day in the various industries due to their exceptional properties. The current commercial production of mullites in industries takes place from the rocks (Toya, Tamura, Kameshima, & Okada, 2004), which is laborious, energy intensive and also an expensive process. Besides this, it is also produced in the laboratory by executing any of these methods i.e. sintering of raw materials of Al, and Si carbide, organic precursors, a sol-gel technique (Jurado, Arévalo Hernández, & Rocha-Rangel, 2013; Won & Siffert, 1998), and chemical vapor deposition (Mulpuri & Sarin, 2011). But, as all the approaches

require expensive instruments and high amount of energy due to which they are not cost-effective, there is a demand of an economical, reliable source of aluminosilicate (Yadav & Fulekar, 2020) rich minerals suitable for mullite synthesis. One such material is fly ash which is rich in aluminosilicates, that comprises of lesser amount of ferrous and other alkali metal oxides (Prochon et al., 2020). Fly ash, is an industrial by product produced during electricity production in thermal power plants (Kumar Yadav & Fulekar, 2019). Fly ash comprises of several toxic heavy metals, present in nano- and micro-sizes that are considered as hazardous, so its disposal is a major challenge globally (Kumar Yadav & Fulekar, 2019)(Yadav & Fulekar, 2018). Generally, fly ash cenospheres are most preferred for the synthesis of mullites as they have less iron oxides (Kumar, Agrawal, & Dhawan, 2020). Numerous investigators have reported the presence of mullite phases while some have reported their synthesis from fly ash under optimized conditions i.e. Jiann-Yang Hwang et al., Beiyue Ma et al., Guihong Han et al., Yingchao Dong et al., concluded that the fly ash based synthesized mullite have an almost similar quality to that of commercial mullite (Fu et al., 2019; Gao, Zhang, Zhang, Sun, & Wang, 2019; Han et al., 2018; Hwang, Huang, & Hein, 1994; Ma et al., 2019).

In the present research work, we have reported the one step extraction of mullite from fly ash by using hydrofluoric acid at room temperature. Moreover, we have also depicted the recovery of most of the metals present in the fly ash in single step by using hydrofluoric acid (HF), which may be processed further for the recovery of elements in their pure form. The extracted mullite and the dried leachate were then analyzed by the X-ray diffraction (XRD), Fourier transform-infrared (FTIR), Field Emission Scanning Electron microscopy (FESEM), Electron diffraction spectroscopy (EDS) and X-ray fluorescence (XRF) for the confirmation of the mullite phase and detection of elements in the leachate respectively.

## 2. MATERIALS AND METHODS

### 2.1 Sampling Area

The fly ash was directly collected from the electrostatic precipitators in to the plastic silos from thermal power plant, Gandhinagar, Gujarat, India. Further the fly ash was dried in an oven at 105 °C before the analysis.

### 2.2. Materials

Fly ash, Neodymium magnet circular shape (4 cm diameter, 0.5 cm height), PTFE beakers (100-200 ml), Milli-Q water, Petri plate, PTFE conical flask, Hydrofluoric acid (Merck, India), Concentrated HCl, concentrated HNO<sub>3</sub>, and Ethylene diamine tetra amine (EDTA)

### 2.3 Recovery of Mullite from Fly Ash

A slurry was prepared by mixing fly ash with distilled water in the ratio of 1: 10, to which a strong neodymium magnet was used for the separation of ferrous fractions from fly ash slurry. The ferrous free fly ash residue was dried in an oven at 60 °C for 6 hours and the residue was mixed with diluted hydrofluoric acid (HF) i.e. 3% by adding 100 mg of fly ash with 2.5 ml HF in a conical flask. Further the mixture was stirred continuously for 15 hours by using Teflon coated magnetic bars on a stirrer at room temperature. After the completion of the reaction, the mixture was centrifuged at 5000 rpm for 5 minutes in a polypropylene centrifuge tubes. The supernatant was decanted and collected in a polypropylene Petri-plate while the solid residue was collected separately. The obtained solid residue was washed several times with distilled water to remove any surface moieties in the form of HF. This residue was washed with dilute HCl (4N), followed by dilute HNO<sub>3</sub> (4N) and EDTA (4N).

The residues obtained during washing from all the liquid was mixed and washed at pH 7 and 9. Similar method was previously applied by the Gomes and Francois in 1999, for the synthesis of mullites from silica rich fly ash (Gomes & François, 2000). The residue was dried in an oven at 70

Figure 1. Schematic diagram: steps involved in the recovery of mullite from fly ash

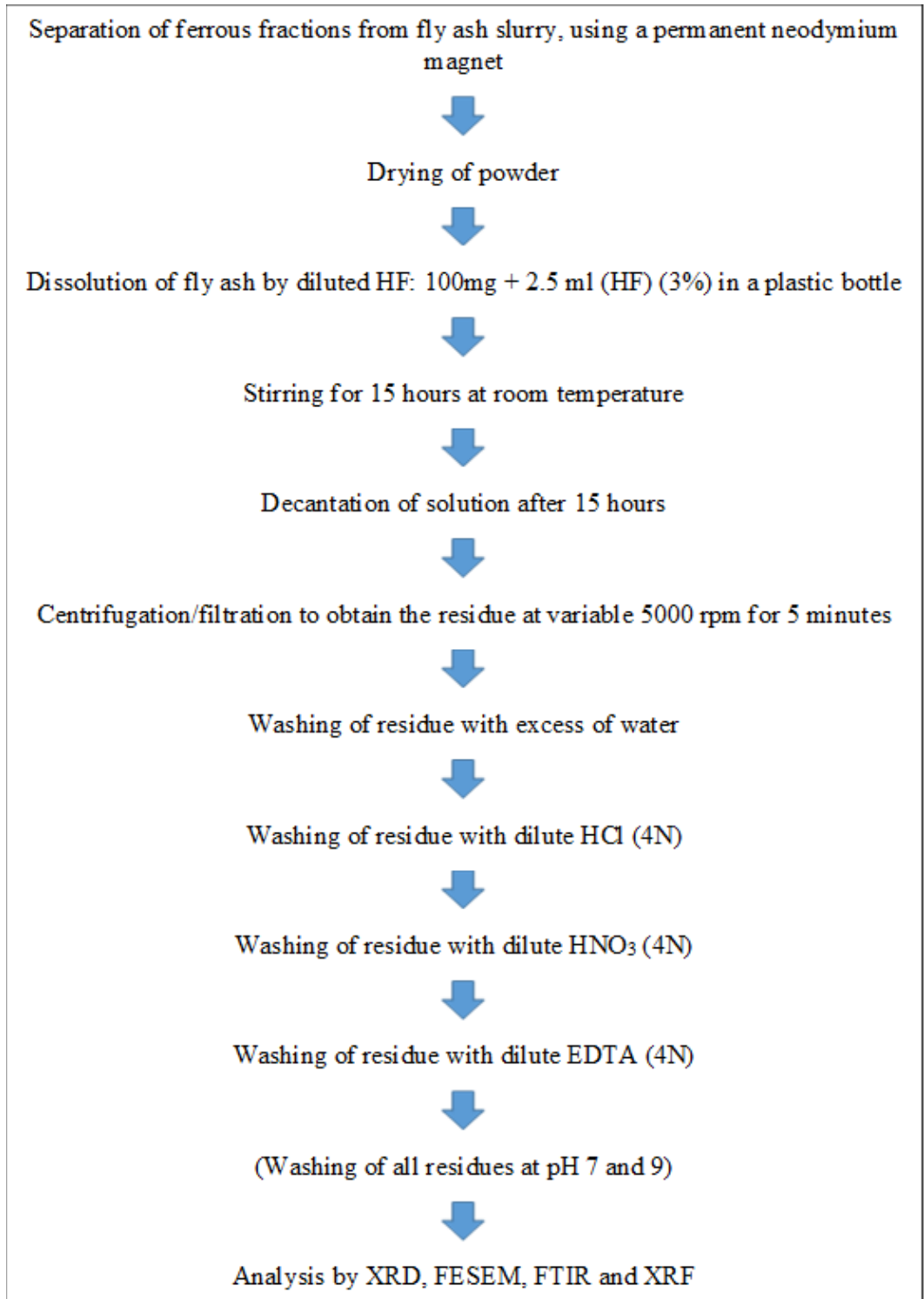
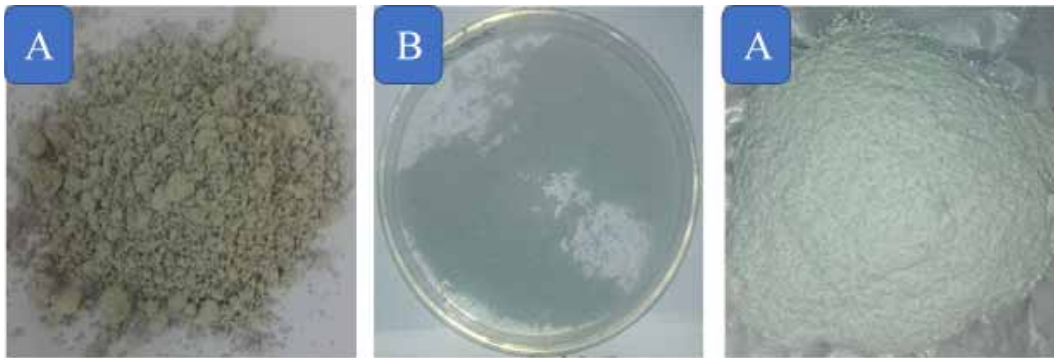


Figure 2. Digital images of a) fly ash, b) mullite and c) dried leachate



°C for overnight. The weight of the obtained residue was noted down and weight loss was calculated from the initial sample. There was about 72% weight loss in the original fly ash sample for which the diagram is shown below in Figure 2. Finally, the sample was analyzed by the sophisticated instruments for the detailed properties of the synthesized sample, as shown above in Figure 1.

### 3. CHARACTERIZATION OF MULLITES

The extraction of mullites from fly ash can be confirmed by a series of characterization techniques that confirm and describe the detail properties of mullite. The techniques like XRF, XRD, FTIR, and FESEM-EDS had an important role in the mullite investigation.

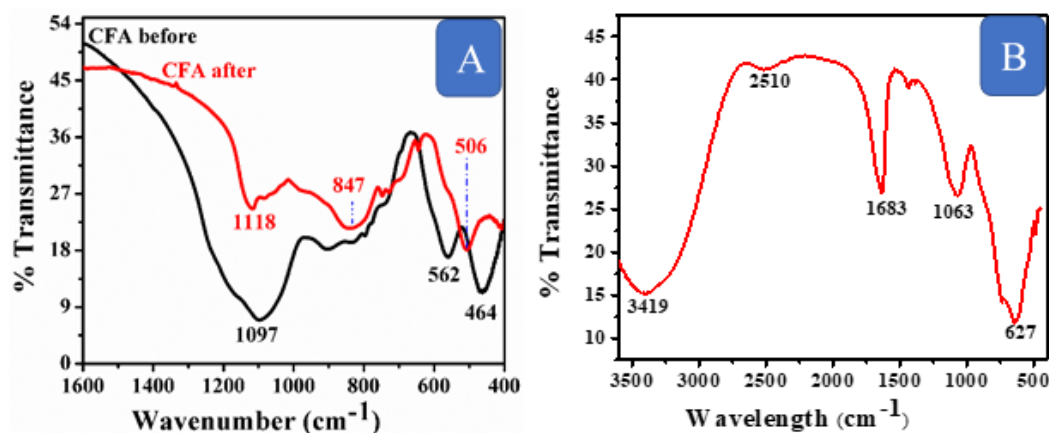
#### 3.1. X-Ray Florescence Spectroscopy

The chemical composition of CFA and dried leachate was analyzed by XRF, using Horiba, Japan make and model no. XGT-2700 X-ray analytical microscope fitted with High purity silicon detector (XEROPHY) X-ray tube with Rh target. For analysis about 5-8 grams of both the samples were mixed separately with the barium chloride and a pellet was prepared for the identification of major elemental oxides. FT-IR spectra was obtained by KBr pellet technique, where ferrous particles were mixed with KBr in appropriate ratio, and a pellet was prepared by using a mechanical pellet making machine. The measurement of the sample was taken against the blank KBr pellet in the infrared region of  $400\text{-}4000\text{ cm}^{-1}$  at a resolution of  $2\text{ cm}^{-1}$  by using Perkin-Elmer one, 6500 spectrum instrument. The XRD patterns were recorded using a Bruker made instrument equipped X'celerator. The XRD patterns were recorded in the  $2\theta$  of  $20\text{-}70^\circ$  with a step size of 0.02 and a time of 5 seconds per step at 40 kV voltage and a current of 30 mA. The phase identification and confirmation of mullite phase was done by the XRD. The morphological analysis of fly ash, mullite and dried leachate particles were carried out by the FESEM model Novo NANOSEM, Carl Zeiss. The dried particles was loaded on the carbon tape which in turn was placed on an aluminum stub holder. The sample was analyzed after the gold sputtering. The EDS analysis of fly ash, mullite and dried leachate was analyzed by Oxford made EDS analyzer attached with the FESEM by focusing the beam on a specific spot of fly ash, mullite and dried leachate particles at variable magnifications and at 20 kV.

### 4. RESULTS AND DISCUSSION

Fly ash have aluminosilicates in the form of mullite and sillimanites (Luo et al., 2017). The inert and crystalline mullite are leached out from the fly ash by strong HF. While the all glassy amorphous

Figure 3. FTIR spectra of fly ash and mullite [A] and dried leachate [B]



forms gets dissolved in the HF and present in the aqueous form (Guo, Liu, Xu, Xu, & Wang, 2010). All the metals reacts with the HF and forms the respective metal fluorides.

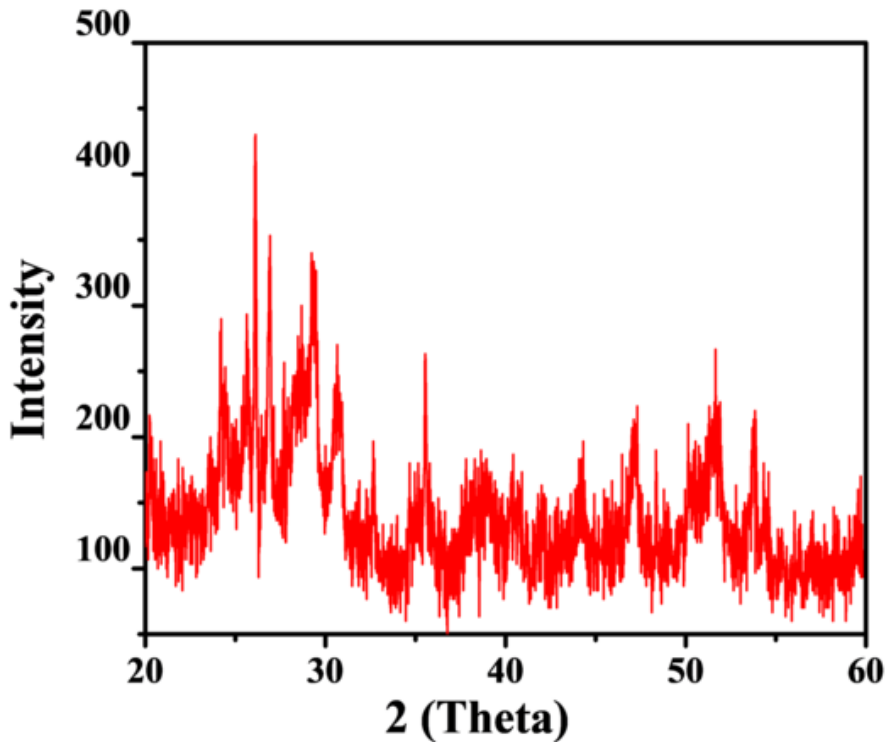
#### 4.1 FTIR Analysis of Fly Ash and Mullite

The FTIR spectra of a typical fly ash particle and mullite is shown in the Figure 3A. The FTIR spectra of fly ash exhibits characteristic bands in the region of 400-1200  $\text{cm}^{-1}$ . The bands at 464  $\text{cm}^{-1}$  and 562  $\text{cm}^{-1}$  is attributed to the Al-O-Si/ Al-O-Al present in the aluminosilicates present in fly ash. These aluminosilicates represents the mullite and cristabolite which are crystalline in nature. Besides this the band at 464  $\text{cm}^{-1}$  is also attributed to the Fe-O band present in the magnetite and hematite in the fly ash. While the band at 1097  $\text{cm}^{-1}$  is attributed to the silicates i.e. Si-O-Si in the fly ash in the form of crystalline and amorphous glassy phase. While a broad band near 3400  $\text{cm}^{-1}$  is not shown over here is attributed to -OH molecule in the fly ash.

While the FTIR spectra in the region of 500-1200  $\text{cm}^{-1}$  is assigned to the mullite structure. The band at 506  $\text{cm}^{-1}$  is attributed to the Si-O-Si/Al-O stretching vibration mode arising from the  $\text{AlO}_6$  groups of mullite (Gören, Ersoy, Özgür, & Alp, 2012). This band got shifted in the mullite from the fly ash towards higher wavenumber. While this band was more sharp in the fly ash which got weakened in the mullite. This indicates the breakage or dissociation of the aluminosilicate structure in the fly ash after HF treatment and formation of mullite from the same. While the band at 847  $\text{cm}^{-1}$  in the mullite is attributed to the  $\text{AlO}_4$  bond. While the band at 1118  $\text{cm}^{-1}$  is attributed to the vibrational mode of the asymmetric stretch of Si-O-Si/silicates in the mullite. All these bands supports the amorphous form of the synthesized mullite (Gören et al., 2012). The band at 3400  $\text{cm}^{-1}$  is attributed to the -OH group present in the particle or might be due to the water molecule. The results obtained were similar to the results reported by Remzi Goren et al (Gören et al., 2012).

Figure 3B reveals FTIR spectra of the dried leachate obtained after treatment of fly ash with the HF. The FTIR spectra characteristic bands at 627, 1063, 1683, 2510 and 3419  $\text{cm}^{-1}$ . The band at 627  $\text{cm}^{-1}$  is attributed to the Si-O-Al of mullite or F-O formed in the leachate. While the band at 1063 is attributed to the Si-O-Si/silicates in the particle. The band at 2510  $\text{cm}^{-1}$  is attributed to the atmospheric carbon dioxide adsorbed by the molecule. A sharp band at 1683  $\text{cm}^{-1}$  is attributed to the OH stretching vibrations, while a broad band at 3419  $\text{cm}^{-1}$  is attributed to the deformation vibration of adsorbed water molecule on the surface of dried leachate (Gören et al., 2012). This could be due to the improper drying of the sample.

Figure 4. XRD pattern of mullite synthesized from fly ash



#### 4.2 XRD Analysis of Fly Ash and Mullite

Fly ash are multifaceted material consisted of alumina, silica and iron, in the forms of mullite, quartz, magnetite, hematite, cristabolite etc. (Yadav & Fulekar, 2020). XRD have  $2\theta$  peaks at 26.27, and 41.12 with d-spacing at 3.328 Å and 2.19 Å were apparent in the graphs confirming the crystalline phase of fly ash.

Besides this, fly ash also showed  $2\theta$  peaks at 26.78, 50.018, and 60.86 for quartz phase, while peaks at 33.53, and 35.49 confirms the presence of iron oxides like hematite and magnetite with fly ash content in the sample. The XRD spectra of mullite in the Figure 4 represented the significant  $2\theta$  two maximal frequencies peak in the range of 23-27 and at 52-53 respectively, corresponding to primary mullite growth and secondary mullite nucleation, confirming the extraction of mullites from the fly ash. The sharp decrease in the silicates peak, mullites indicates that the majority of the glassy amorphous phase of silica removed with the HF treatment. These glassy phase represents the vitreous phase of the fly ash due to which mainly applied in the ceramics. Similar peaks were also obtained by the Gomes and Francois (Gomes & François, 2000). Similar XRD diffractograms was also obtained by Gong et al, and Amigo et al (Amigó et al., 2005; L. Gong et al., 2014).

#### 4.3 FESEM-EDS for Morphological Analysis

Figure 5a shows FESEM micrograph of fly ash particles. The particles are spherical shaped whose size is varying from 0.2-7 microns. While the Figure 5b is EDS spectra and elemental composition

of fly ash particles. The EDS-spectra of fly ash confirmed the presence of O, Al, Si, C, Fe, Ti, Mg, Ca, K as prominent peaks were evident within the micrograph regarding the same.

However, the quantitative presence of O was found four times of Al and Si oxides and Al and Si oxides were present as second and third profuse oxide with in the sample. The relative presence of these oxides indicated the classical composition of mullite in the silico-aluminous fly ash sample having marginally enriched Al oxides in it (Choo, Mohd, Kok, & Matori, 2019; Gomes & François, 2000). Remaining elements like C, Fe, Ti, Mg, Ca, and K were found in trace amount within the fly ash. Still, they contribute to the characteristic property of the sample same way as the presence of Fe and Mg oxides denoted the enhanced stability of the sample (Setoodeh Jahromy et al., 2019). Fe and Mg are considered to provide good stability to the silico-aluminous fly ashes (Bénézet, Adamiec, & Benhassaine, 2008). Moreover, the low quantity of elementary calcium denoted the low calcium siliceous nature of the fly ash sample (Singh & Subramaniam, 2018).

While, Figure 5C-F shows FESEM micrographs of mullite particles recovered from the fly ash. The particles are needle-shaped micron sized (Zhu, Dong, Li, Liu, & You, 2015) having 1-1.5 microns length and 0.3-0.5 microns width (a/e). Zhu et al and Gomes and Francois also obtained needle shaped mullite particles from fly ash during HF treatment of fly ash (Gomes & François, 2000; Zhu et al., 2015).

Furthermore, agglomerated tiny spherical particles were also evident in the micrographs clustering around the needle-shaped micron representing smaller granules of different elements. The Figure 5G shows the EDS spot of the mullite particles while the EDS spectra of mullite particles in Figure 5H documented C, O, Al, Si, and F peak. The carbon was verified in the highest amount following the rest. While the Al, Si, O and C were considered the part of the elementary composition of fly ash whereas the presence of fluorine is denoted as the impurity.

Figure 6A-D shows, FESEM micrographs of the dried leachate powders during treatment of fly ash with diluted HF. The FESEM micrographs revealed an octahedral or hexagonal block-shaped agglomerated particles having size in the range of 300 nm-1 micron. The Fluorine was apparent in the micrograph (A). Tiny granules of different element like Na, Al, and Si were considered to be present on the surface of fluorine particles in agglomerated forms (B). Granules present over the surface can be easily distinguished in two categories; white spherical shaped nanoparticles representing the Na (D) and rest smaller than these, agglomerated granules of fly ash elementary composition. EDS-spectra also revealed the highest presence of Fluorine element. Besides it Na, C, Si, O and Al were exhibited in the spectra.

#### 4.4 XRF Analysis of Fly Ash and Dried Leachate

XRF helped in the quantitative analysis of elements present in the oxides form in both fly ash and dried leachate. The composition of major elements in the oxides form of coal fly ash (CFA) and dried leachate (DL) are given in the Table 1.

The major elemental oxides of CFA is silica ( $\text{SiO}_2$ ), alumina ( $\text{Al}_2\text{O}_3$ ), ferrous ( $\text{Fe}_2\text{O}_3$ ), sodium dioxide ( $\text{Na}_2\text{O}$ ) and titanium dioxide ( $\text{TiO}_2$ ) which alone comprises 96.6% and the remaining 3.4% is constituted by oxides of Ca, Mg, Na, K and P. The silica content is 56.98%, alumina 27.07% and ferrous oxides is 5.4%, so the total ferro-aluminosilicates content is 89.4% in the CFA. Figure 6E shows the EDS spot for retrieving the elemental analysis of the mullite. Even if CaO would be included, then this value will reach to 90.4%. Besides this, CFA also have CuO (0.2%) and SrO (0.02%) as toxic heavy metal oxides. While the major elemental oxides in the dried leachate obtained from HF treatment of fly ash have alumina i.e. 54.45%, ferrous 16.73%, silica 6.04%, calcium oxide 5.18%, rutile 5.82 while rest were comprised of oxides of P, K, Mg, Na, Mn, Cu, Sr and sulphur shown in Figure 7. This clearly indicates that, after HF treatment almost 85-90% silica was recovered, while the alumina content increased to more than two folds. This could be due to the breakage of aluminosilicate bond in the fly ash by the strong acid HF that could have released into the aqueous solutions during treatment. As, the breakage of aluminosilicate bonds was also evident by the FTIR and XRD analysis, the ferrous



Figure 5. FESEM micrographs (a) and EDS spectra (b) of fly ash particles, (A-D) EDS spot (E) and EDS spectra of fly ash mullites (F), whereas Figure 5B reprinted from Yadav and Fulekar 2019 (Kumar Yadav & Fulekar, 2019).

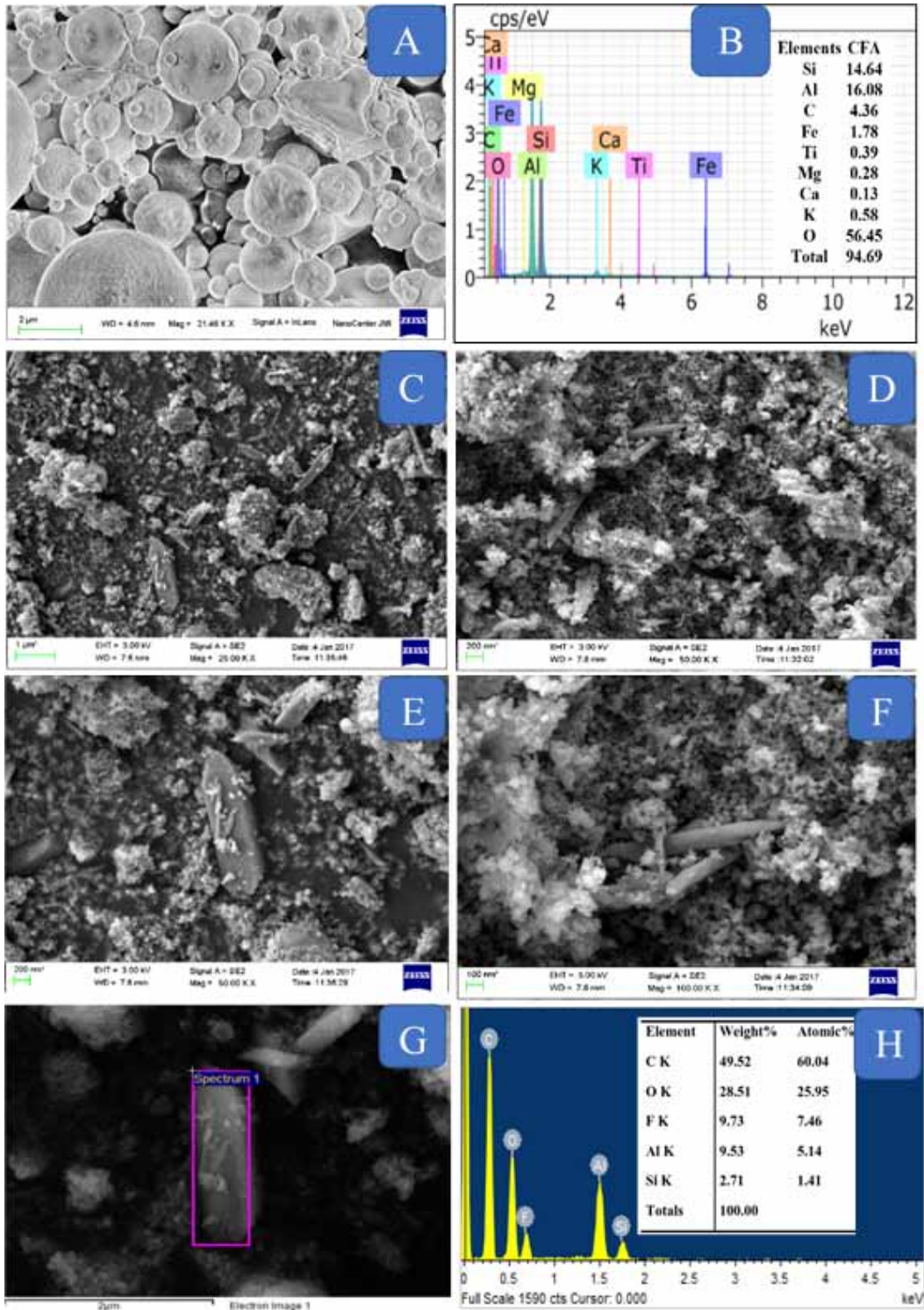
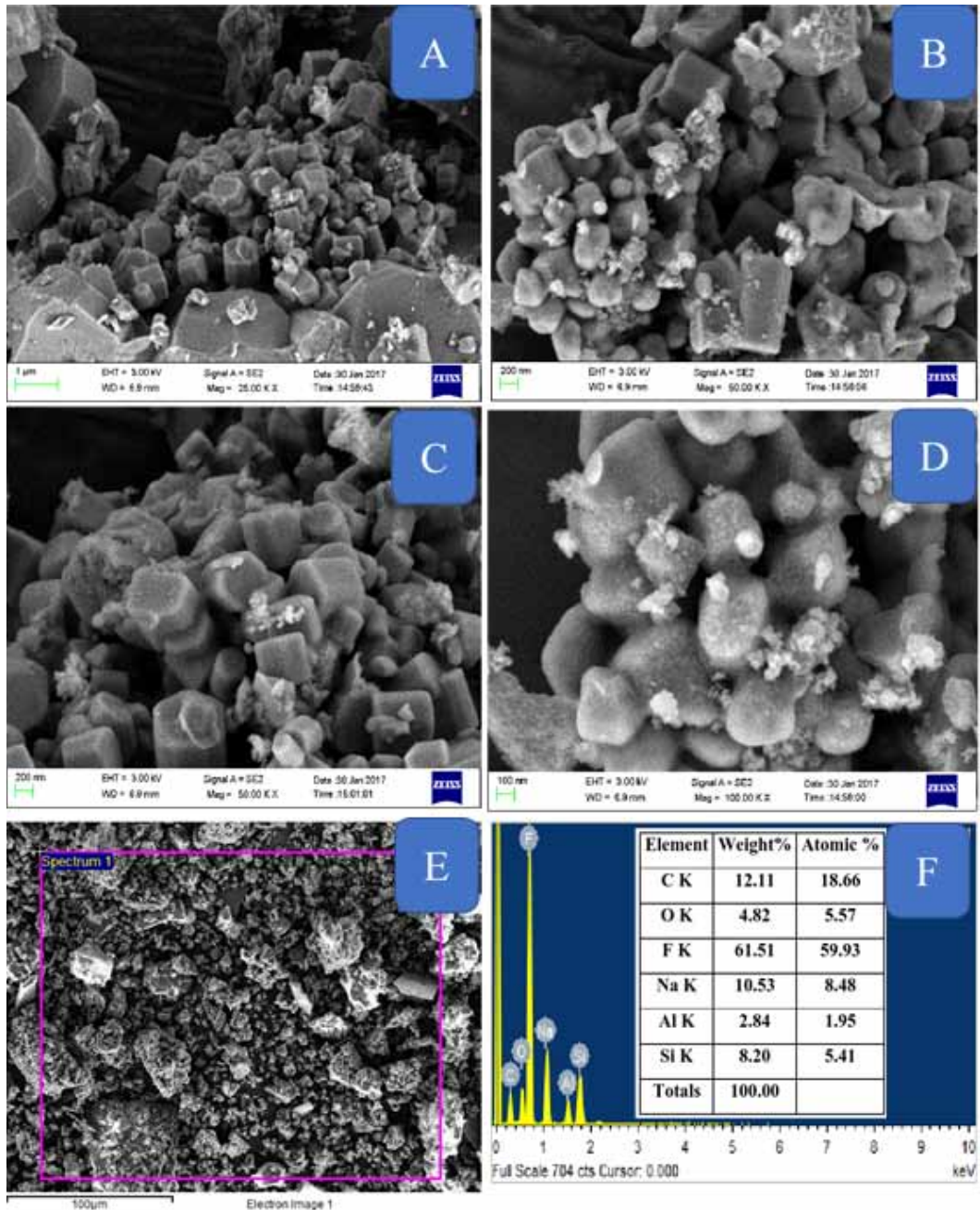
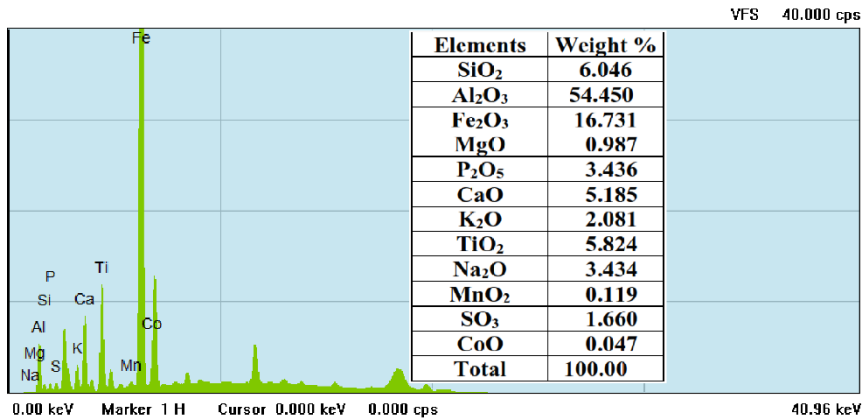


Figure 6. FESEM micrographs (A-D) EDS spot (E) and EDS spectra dried leachate powders (F)



content slightly increased into the dried leachate. Whose possible explanation could be due to the presence of Fe in the form of ferro-alumino-silicate minerals in the fly ash, which on dissociation by HF liberated free into the solution. Though, the ferrous was initially extracted from the fly ash by external magnet, these ferrous arrived from the internal structure which was initially not available freely in the fly ash. Moreover, the rutile and CaO content increased into the dried leachate more

Figure 7. XRF spectra and elemental composition of dried leachate



than tenfold and six fold respectively. Apart from this, increase in the content was also seen for P, K, Na, Mn, S, Cu, and Sr after HF treatment. This indicates that most of the elements were initially in the bounded form in the fly ash, which got liberated after HF treatment into the aqueous solution. There was only MgO whose value decreased after the HF treatment.

## 5. CONCLUSION

The current research work reported the extraction of mullite from fly ash along with the extraction of the important major elements. The extracted mullite was analyzed by the sophisticated instruments that revealed their spindle shape having size 1-3 microns in length and 0.1-0.3 microns in width.

Table 1. Chemical composition of fly ash and dried leachate residue by XRF

Elements	Value	
	CFA (%)	DL (%)
SiO <sub>2</sub>	46.017	6.04
Al <sub>2</sub> O <sub>3</sub>	25.823	54.45
Fe <sub>2</sub> O <sub>3</sub>	15.938	16.73
MgO	7.455	0.98
P <sub>2</sub> O <sub>5</sub>	1.524	3.43
CaO	0.759	5.18
K <sub>2</sub> O	0.724	2.08
TiO <sub>2</sub>	0.544	5.82
Na <sub>2</sub> O	0.352	3.43
MnO <sub>2</sub>	0.039	0.12
SO <sub>3</sub>	0.04	3.77
CuO	0.20	0.87
SrO	0.02	0.16
Total	100.67	99.99

The recovery of mullite from such industrial waste may act as a sustainable and economical source. Moreover, the dried residue could be processed further for the recovery of value added minerals. The suggested method not only minimizes the pollution but also recycles the fly ash into a value added minerals.

## **ACKNOWLEDGMENT**

The authors are also thankful to the Central Instrumental facility (CIF) of Central University of Gujarat, CIF- Centre for Nanosciences, Jamia Millia Islamia, New Delhi, CECRI (CSIR)-Karikudi, Tamil Nadu.

## REFERENCES

- Aksel, C. (2003). The Effect of Mullite on the Mechanical Properties and Thermal Shock Behavior of Alumina-Mullite Refractory Materials. *Ceramics International*, 29(2), 183–188. doi:10.1016/S0272-8842(02)00103-7
- Amigó, J. M., Serrano, F. J., Kojdecki, M. A., Bastida, J., Esteve, V., Reventós, M. M., & Martí, F. (2005). X-ray diffraction microstructure analysis of mullite, quartz and corundum in porcelain insulators. *Journal of the European Ceramic Society*, 25(9), 1479–1486. doi:10.1016/j.jeurceramsoc.2004.05.019
- Anggono, J. (2005). Mullite Ceramics: Its Properties, Structure, and Synthesis. *Jurnal Teknik Mesin*, 7(1).
- Baspinar, M. S., & Kara, F. (2009). Optimization of the Corrosion Behavior of Mullite Refractories against Alkali Vapor Vvia ZrSiO<sub>4</sub> Addition to the Binder Phase. *Ceramics-Silikáty*, 53(4).
- Bénézet, J. C., Adamiec, P., & Benhassaine, A. (2008). Relation between silico-aluminous fly ash and its coal of origin. *Particuology*, 6(2), 85–92. doi:10.1016/j.partic.2007.09.002
- Chen, C.-Y., Lan, G., & Tuan, W. (2000). Preparation of Mullite by the Reaction Sintering of Kaolinite and Alumina. *Journal of the European Ceramic Society*, 20(14), 2519–2525. doi:10.1016/S0955-2219(00)00125-4
- Choo, M., Mohd Salleh, , Kok, , & Matori, . (2019). A Review on Synthesis of Mullite Ceramics from Industrial Wastes. *Recycling*, 4(3), 39. doi:10.3390/recycling4030039
- Choo, T. F., Mohd Salleh, M. A., Kok, K. Y., Matori, K. A., & Abdul Rashid, S. (2020). Characterization of High-Temperature Hierarchical Porous Mullite Washcoat Synthesized Using Aluminum Dross and Coal Fly Ash. *Crystals*, 10(3), 178. doi:10.3390/cryst10030178
- Cui, K., Zhang, Y., Fu, T., Wang, J., & Zhang, X. (2020). Toughening Mechanism of Mullite Matrix Composites: A Review. *Coatings*, 10(7), 672. doi:10.3390/coatings10070672
- Eom, J.-H., Kim, Y.-W., & Raju, S. (2013). Processing and properties of macroporous silicon carbide ceramics: A review. *Journal of Asian Ceramic Societies*, 1(3), 220–242. doi:10.1016/j.jascer.2013.07.003
- Fischer, R., Gaede-Köhler, A., Birkenstock, J., & Schneider, H. (2012). Mullite and Mullite-Type Structures. *International Journal of Materials Research*, 103(4), 402–407. doi:10.3139/146.110713
- Fu, M., Liu, J., Dong, X., Zhu, L., Dong, Y., & Hampshire, S. (2019). Waste recycling of coal fly ash for design of highly porous whisker-structured mullite ceramic membranes. *Journal of the European Ceramic Society*, 39(16), 5320–5331. doi:10.1016/j.jeurceramsoc.2019.08.042
- Gao, S., Zhang, Y., Zhang, Y., Sun, S., & Wang, M. (2019). Study on the extracted process of mullite from coal fly ash by-product sodium silicate. *Journal of the Ceramic Society of Japan*, 127(2), 90–97. doi:10.2109/jcersj2.18067
- Gomes, S., & François, M. (2000). Characterization of mullite in silicoaluminous fly ash by XRD, TEM, and <sup>29</sup>Si MAS NMR. *Cement and Concrete Research*, 30(2), 175–181. doi:10.1016/S0008-8846(99)00226-4
- Gong, L., Wang, Y., Cheng, X., Zhang, R., & Zhang, H. (2014). Porous mullite ceramics with low thermal conductivity prepared by foaming and starch consolidation. *Journal of Porous Materials*, 21(1), 15–21. doi:10.1007/s10934-013-9741-z
- Gong, Y., Sun, J., Sun, S.-Y., Lu, G., & Zhang, T.-A. (2019). Enhanced Desilication of High Alumina Fly Ash by Combining Physical and Chemical Activation. *Metals*, 9(4), 411. doi:10.3390/met9040411
- Gören, R., Ersoy, B., Özgür, C., & Alp, T. (2012). Colloidal stability–slip casting behavior relationship in slurry of mullite synthesized by the USP method. *Ceramics International* -. *Ceramics International*, 38(1), 679–685. doi:10.1016/j.ceramint.2011.07.056
- Guo, A., Liu, J., Xu, R., Xu, H., & Wang, C. (2010). Preparation of Mullite from Desilication-Flyash. *Fuel*, 89(12), 3630–3636. doi:10.1016/j.fuel.2010.07.042
- Han, G., Yang, S., Peng, W., Huang, Y., Wu, H., Chai, W., & Liu, J. (2018). Enhanced recycling and utilization of mullite from coal fly ash with a flotation and metallurgy process. *Journal of Cleaner Production*, 178, 804–813. doi:10.1016/j.jclepro.2018.01.073

- Hwang, J.-Y., Huang, X., & Hein, A. M. (1994). Synthesizing mullite from beneficiated fly ash. *JOM*, 46(5), 36–39. doi:10.1007/BF03220694
- Igo, A. V. (2019). Determination of the Crystallization Temperature of Mullite by Luminescence Spectra of Europium and Chromium Ions. *Physics of the Solid State*, 61(12), 2434–2437. doi:10.1134/S1063783419120163
- Jurado, L. T., Arévalo Hernández, R. M., & Rocha-Rangel, E. (2013). Sol-Gel Synthesis of Mullite Starting from Different Inorganic Precursors. *Journal of Powder Technology*, 268070, 1–7. Advance online publication. doi:10.1155/2013/268070
- Kamara, S., Wei, W., & Ai, C. (2020). Fabrication of Refractory Materials from Coal Fly Ash, Commercially Purified Kaolin, and Alumina Powders. *Materials (Basel, Switzerland)*, 13(15), 15. doi:10.3390/ma13153406 PMID:32748818
- Kumar, A., Agrawal, S., & Dhawan, N. (2020). Processing of Coal Fly Ash for the Extraction of Alumina Values. *Journal of Sustainable Metallurgy*, 6(2), 294–306. doi:10.1007/s40831-020-00275-6
- Kumar Yadav, V., & Fulekar, M. H. (2019). Green synthesis and characterization of amorphous silica nanoparticles from fly ash. *Materials Today: Proceedings*, 18(Part 7), 4351–4359. doi:10.1016/j.matpr.2019.07.395
- Laita, E., Bauluz, B., & Yuste, A. (2019). High-Temperature Mineral Phases Generated in Natural Clinkers by Spontaneous Combustion of Coal. *Minerals (Basel)*, 9(4), 213. doi:10.3390/min9040213
- Li, D. X., & Thomson, W. J. (1991). Mullite Formation from Nonstoichiometric Diphasic Precursors. *Journal of the American Ceramic Society*, 74(10), 2382–2387. doi:10.1111/j.1151-2916.1991.tb06772.x
- Liu, Y., Huang, J. F., Wang, X. F., Yang, Q., Wang, Y. Q., Rao, P. W., & Wang, Q. G. (2011). Research on the High Strength Glass Ceramics/Mullite Ceramics Composites. *New Journal of Glass and Ceramics*, 01(02), 53–57. doi:10.4236/njgc.2011.12009
- Luo, Y., Yang, L., Zheng, S., Liu, C., Han, D., & Xiaohui, W. (2017). Mullite-based ceramic tiles produced solely from high-alumina fly ash: Preparation and sintering mechanism. *Journal of Alloys and Compounds*, 732, 828–837. doi:10.1016/j.jallcom.2017.09.179
- Ma, B., Su, C., Ren, X., Gao, Z., Qian, F., Yang, W., Liu, G., Li, H., Yu, J., & Zhu, Q. (2019). Preparation and properties of porous mullite ceramics with high-closed porosity and high strength from fly ash via reaction synthesis process. *Journal of Alloys and Compounds*, 803(16), 981–991. doi:10.1016/j.jallcom.2019.06.272
- Martin-Marquez, J., & Romero, M. (2010). Mullite development on firing in porcelain stoneware bodies. *Journal of the European Ceramic Society*, 30(7), 1599–1607. doi:10.1016/j.jeurceramsoc.2010.01.002
- Mulpuri, R. P., & Sarin, V. K. (2011). Synthesis of mullite coatings by chemical vapor deposition. *Journal of Materials Research*, 11(6), 1315–1324. doi:10.1557/JMR.1996.0166
- O'Connor, S., Mackenzie, K., Smith, M., & Hanna, J. (2010). Ion exchange in the charge-balancing sites of aluminosilicate inorganic polymers. *Journal of Materials Chemistry*, 20(45), 10234–10240. doi:10.1039/c0jm01254h
- Ohtake, T., Uchida, K., Ikazaki, F., Kawamura, M., Ohkubo, T., & Kamiya, K. (1991). Synthesis of Mullite from Fly Ash and Alumina Powder Mixture. *Journal of the Ceramic Society of Japan*, 99(1147), 239–243. doi:10.2109/jcersj.99.239
- Oikonomou, P., Dedeloudis, C., Stournaras, C. J., & Ftikos, C. (2007). Stabilized tialite–mullite composites with low thermal expansion and high strength for catalytic converters. *Journal of the European Ceramic Society*, 27(12), 3475–3482. doi:10.1016/j.jeurceramsoc.2006.07.020
- Pasek, M., Block, K., & Pasek, V. (2012). Fulgurite Morphology: A Classification Scheme and Clues to Formation. *Contributions to Mineralogy and Petrology*, 164(3), 477–492. doi:10.1007/s00410-012-0753-5
- Prochon, P., Zhao, Z., Courard, L., Piotrowski, T., Michel, F., & Garbacz, A. (2020). Influence of Activators on Mechanical Properties of Modified Fly Ash Based Geopolymer Mortars. *Materials (Basel, Switzerland)*, 13(5), 1033. Advance online publication. doi:10.3390/ma13051033 PMID:32106414
- Sadik, C., Amrani, I.-E. E., & Albizane, A. (2014). Processing and characterization of alumina–mullite ceramics. *Journal of Asian Ceramic Societies*, 2(4), 310–316. doi:10.1016/j.jascer.2014.07.006



Sadik, C., El Amrani, I.-E., & Albizane, A. (2014). Recent advances in silica-alumina refractory: A review. *Journal of Asian Ceramic Societies*, 2(2), 83–96. doi:10.1016/j.jascer.2014.03.001

Santos, S., & Rodrigues, J. (2003). Correlation Between Fracture Toughness, Work of Fracture and Fractal Dimensions of Alumina-Mullite-Zirconia Composites. *Materials Research*, 6(2), 219–226. doi:10.1590/S1516-14392003000200017

Schneider, H., Fischer, R., & Schreuer, J. (2015a). Mullite: Crystal Structure and Related Properties. *Journal of the American Ceramic Society*, 98(10), 2948–2967. doi:10.1111/jace.13817

Schneider, H., Fischer, R. X., & Schreuer, J. (2015b). Mullite: Crystal Structure and Related Properties. *Journal of the American Ceramic Society*, 98(10), 2948–2967. doi:10.1111/jace.13817

Schneider, H., Schmücker, M., & MacKenzie, K. J. D. (2005). Basic Properties of Mullite. *Mullite*, 141-225. doi:10.1002/3527607358.ch2 10.1002/3527607358.ch2

Schneider, H., Schreuer, J., & Hildmann, B. (2008). Structure and Properties of Mullite - A Review. *Journal of the European Ceramic Society*, 28(2), 329–344. doi:10.1016/j.jeurceramsoc.2007.03.017

Searle, E. J. (1962). Xenoliths and metamorphosed rocks associated with the Auckland basalts. *New Zealand Journal of Geology and Geophysics*, 5(3), 384–403. doi:10.1080/00288306.1962.10420095

Setoodeh Jahromy, S., Azam, M., Huber, F., Jordan, C., Wesenauer, F., Huber, C., Naghdi, S., Schwendtner, K., Neuwirth, E., Laminger, T., Eder, D., Werner, A., Harasek, M., & Winter, F. (2019). Comparing Fly Ash Samples from Different Types of Incinerators for Their Potential as Storage Materials for Thermochemical Energy and CO<sub>2</sub>. *Materials (Basel, Switzerland)*, 12(20), 3358. doi:10.3390/ma12203358 PMID:31618854

Torreccillas, R., Calderón, J., Moya, J., Reece, M., Davies, C., Olagnon, C., & Fantozzi, G. (1999). Suitability of mullite for high temperature applications. *Journal of The European Ceramic Society - Journal of the European Ceramic Society*, 19(13-14), 2519–2527. doi:10.1016/S0955-2219(99)00116-8

Toya, T., Tamura, Y., Kameshima, Y., & Okada, K. (2004). Preparation and Properties of CaO–MgO–Al<sub>2</sub>O<sub>3</sub>–SiO<sub>2</sub> glass–ceramics from Kaolin Clay Refining Waste (Kira) and Dolomite. *Ceramics International*, 30(6), 983–989. doi:10.1016/j.ceramint.2003.11.005

Treadwell, D. R., Dabbs, D. M., & Aksay, I. A. (1996). Mullite (3Al<sub>2</sub>O<sub>3</sub>–2SiO<sub>2</sub>) Synthesis with Aluminosiloxanes. *Chemistry of Materials*, 8(8), 2056–2060. doi:10.1021/cm960110y

Tripathi, H., Ghosh, A., Halder, M., Mukherjee, B., & Maiti, H. (2012). Microstructure and properties of sintered mullite developed from Indian bauxite. *Bulletin of Materials Science*, 35(4), 639–643. doi:10.1007/s12034-012-0337-z

Uribe, R., Moreno, R., & Baudín, C. (2001). Influence of mullite additions on thermal shock resistance of dense alumina materials. Part 2: Thermal properties and thermal shock behaviour. *British Ceramic Transactions*, 100(6), 246-250. 10.1179/096797801681503

Wang, K., & Sacks, M. (2005). Mullite Formation by Endothermic Reaction of  $\alpha$ -Alumina/Silica Microcomposite Particles. *Journal of the American Ceramic Society*, 79(1), 12–16. doi:10.1111/j.1151-2916.1996.tb07874.x

Won, C.-W., & Siffert, B. (1998). Preparation by sol-gel method of SiO<sub>2</sub> and mullite (3Al<sub>2</sub>O<sub>3</sub>, 2SiO<sub>2</sub>) powders and study of their surface characteristics by inverse gas chromatography and zetametry. *Colloids and Surfaces. A, Physicochemical and Engineering Aspects*, 131(1-3), 161–172. doi:10.1016/S0927-7757(97)00149-0

Yadav, V. K., & Fulekar, M. H. (2018). The current scenario of thermal power plants and fly ash: Production and utilization with a focus in India. *International Journal of Advance Engineering and Research Development*, 5(4), 768–777.

Yadav, V. K., & Fulekar, M. H. (2020). Advances in Methods for Recovery of Ferrous, Alumina, and Silica Nanoparticles from Fly Ash Waste. *Ceramics*, 3(3), 384–420. doi:10.3390/ceramics3030034

Zhu, L., Dong, Y., Li, L., Liu, J., & You, S.-J. (2015). Coal fly ash industrial waste recycling for fabrication of mullite-whisker-structured porous ceramic membrane supports. *RSC Advances*, 5(15), 11163–11174. doi:10.1039/C4RA10912K

*Virendra K. Yadav has expertise in the field of microbial nanosciences and nanoparticles from waste materials.*

*Pallavi Saxena has a Ph.D. in Nanoecotoxicology.*

*Chagan Lal's research interests are nanochemistry, solar cells, and chemistry.*

*Govindhan Gnanamoorthy has expertise in synthesis and characterization of organic and inorganic nanoparticles and electronic applications of doped nanoparticles.*

*Nisha Choudhary's research interests are nanomaterials, wastewater treatment, and nanocomposites.*

*Bijendra Singh has expertise in the field of chemical synthesis of nanoparticles, wastewater treatment, and photochemistry.*

*Neha Tavker completed her Masters in Industrial Chemistry and pursued MPhil-PhD in Nano Sciences. Her major research interests include nanocomposites fabrication, photocatalysis, environmental application, and extraction of natural polymers.*

*Haresh Kalasariya's research interests are microbiology, algae, and GCMS.*

*Pankaj Kumar's research interests are environment, heavy metals, and bioremediation.*